



Soft Matter

**A chiral-racemic lyotropic chromonic liquid crystal system**

Journal:	<i>Soft Matter</i>
Manuscript ID	SM-ART-11-2020-002013
Article Type:	Paper
Date Submitted by the Author:	12-Nov-2020
Complete List of Authors:	Ando, Jordan; Swarthmore College Collings, Peter; Swarthmore College

SCHOLARONE™  
Manuscripts

Cite this: DOI: 00.0000/xxxxxxxxxx

## A chiral-racemic lyotropic chromonic liquid crystal system†

Jordan K. Ando,<sup>a</sup> and Peter J. Collings<sup>a,b,\*</sup>

Received Date

Accepted Date

DOI: 00.0000/xxxxxxxxxx

The two main classes of liquid crystals are thermotropic (containing no solvent) and lyotropic (containing solvent). Both of these classes possess the nematic phase, the most simple of liquid crystal phases with only uniaxial orientational order. For both of these classes, if the constituent molecules are chiral or if a chiral dopant is added, the preferred direction of orientation rotates in helical fashion in what is called the chiral nematic phase. Recent research has shown that because the ordering entities of the two classes are quite different (molecules versus molecular assemblies), important differences in the properties of the nematic phase can result. While thermotropic chiral nematics have been extensively examined, less is known about lyotropic chiral nematics, especially for the most ideal case, a chiral-racemic system. Furthermore, none of the lyotropic chiral-racemic studies has included lyotropic chromonic liquid crystals, which are solutions of dyes, drugs, and nucleic acids. Inverse pitch measurements are reported for a chiral-racemic system of a chromonic liquid crystal across the entire chiral fraction range and over a 30°C temperature interval. The inverse pitch depends linearly on chiral fraction and decreases with increasing temperature, indicating that achiral and chiral molecules participate in the assembly structure similarly. The helical twisting power is significantly larger than for other chiral lyotropic liquid crystals due to the very high scission energy of the investigated system.

## 1 Introduction

The liquid crystal phase of matter consists of entities that spontaneously order orientationally and sometimes positionally as well. The ordered entities in a thermotropic liquid crystal are molecules or associations of molecules, and there is no solvent. In lyotropic liquid crystals, the ordered entities are molecular assemblies that form in the presence of a solvent. The most simple liquid crystal phase is the nematic phase, in which the ordered entities maintain only orientational order as they diffuse throughout the material. Both thermotropic and lyotropic liquid crystals form the nematic phase, and although they possess the same macroscopic symmetry, recent investigations have uncovered some important differences. A good example is the elastic behavior, for which twist deformations are significantly less costly energetically in lyotropic compared to thermotropic liquid crystals. Thus when the nematic phase is forced to deform due to confinement, lyotropic liquid crystals exhibit twist deformation much more frequently than thermotropic liquid crystals. This propensity toward twist

deformation seems to be true for all lyotropic liquid crystals, regardless of whether the ordering entities are polymers, micelles, or stacks of chromonic molecules or short DNA oligomers.<sup>1–8</sup>

If chirality is present, either because the ordering entity possesses chirality or if a chiral solute is added, the chiral nematic phase forms. In this phase, the preferred direction of orientational order of the entities rotates in helical fashion. The distance over which the preferred direction rotates 360° is called the pitch, and can be as small as the wavelength of light or as large as the dimensions of the sample container. Chirality is an important property in the field of liquid crystals, and is studied both for fundamental understanding of soft matter phases and for various applications in areas such as optics and chemical sensing.

Theoretical and experimental research on chiral thermotropics is vast; similar work on chiral lyotropics has a long history too, but the extent is less. Investigations have utilized both chiral solute molecules added to an otherwise achiral system and intrinsically chiral systems in which the liquid crystal forming molecules themselves are chiral. It is this second case, lyotropic liquid crystals in which the molecules forming the assemblies are chiral, that has not been as widely studied. Solutions of synthetic polypeptides form chiral nematic phases and have been investigated for decades.<sup>9</sup> Micellar liquid crystals formed in solution with chiral dopants or by chiral surfactants have also been the subject of research for many years. One of the earliest studies of “induced”

<sup>a</sup> Department of Physics & Astronomy, Swarthmore College, Swarthmore, PA, U.S.A.

<sup>b</sup> Department of Physics and Astronomy, University of Pennsylvania, Philadelphia, PA, U.S.A.

\* Corresponding Author. Email: pcollin1@swarthmore.edu

† Electronic Supplementary Information (ESI) available: See DOI: 10.1039/cXsm00000x/

chiral micellar lyotropic phases was done by Radley and Saupé, which revealed that chiral nematic phases form just as in thermotropic and polypeptide systems.<sup>10</sup> Research on “intrinsic” chiral lyotropic phases started soon thereafter,<sup>11</sup> and was followed by many investigations into the local ordering in the micelles using new chiral surfactant systems. Refs. 12–16 are representative of the research from this period<sup>12–16</sup> and Refs. 17 and 18 are review articles summarizing it.<sup>17,18</sup> Much more recently, the chiral nematic phase of an intrinsic chiral chromonic liquid crystal has been studied<sup>19–23</sup>. Chromonic liquid crystals are a unique class of lyotropic liquid crystals in which dyes, drugs, and nucleic acids spontaneously form rod-like assemblies that in turn order into a nematic or chiral nematic phase for a certain range of concentration and temperature. The distribution of assembly size in chromonic liquid crystals is extremely wide and strongly depends on both concentration and temperature. This can cause an unusual temperature dependence, for example, a divergence of the pitch as the transition to the isotropic phase is approached.<sup>23</sup> Extremely recently, a study of mixtures of chromonic and micellar compounds revealed a robust phase diagram containing both uniaxial and biaxial nematic phases.<sup>24</sup> Finally, the chiral nematic phase of solutions of short DNA oligomers<sup>25</sup> and cellulose nanocrystals<sup>26</sup> have been investigated.

One of the most useful ways to study chiral liquid crystals is to utilize a chiral-racemic system. With one of the chiral enantiomers and a racemic mixture of both chiral enantiomers on hand, various proportions of the two allow the chirality to be varied while all other parameters of the system remain constant. Often changing the fraction of chiral enantiomer in the mixture results in a linear variation of the inverse pitch. This implies that the opposite enantiomers can substitute for each other without any change in the type or amount of order. However, sometimes at high chirality it is energetically favorable for the molecules of thermotropic liquid crystals to order differently from what occurs in the chiral nematic phase at lower chiral fraction. Three-dimensional networks of line defects form with a more complicated arrangement of the director between them.<sup>27</sup> There has been far fewer chiral-racemic studies involving lyotropic liquid crystals, so much less is known. The inverse pitch was measured for disk-shaped, bilayer, micellar lyotropic liquid crystals and was proportional to chiral fraction across the entire range.<sup>13,15</sup> A more recent study of two disk-shaped, bilayer, micellar lyotropic liquid crystals examined the structure of the micelles using x-ray scattering.<sup>28</sup>

Inverse pitch and transition temperature measurements on a chiral-racemic system of the intrinsic chiral lyotropic chromonic liquid crystal 2-Aminomethyl-1-ethylpyrrolidine 3,4,9,10-perylenebis-(dicarboximide) HCl salt are reported. Measurements extend over the entire chiral fraction range and 30°C of temperature. The helical twisting power of the chiral enantiomer is significantly larger than for other lyotropic chiral nematics and decreases with an increase in temperature.

## 2 Experimental methods

Chiral and racemic samples of the chromonic liquid crystal precursor 2-Aminomethyl-1-ethylpyrrolidine 3,4,9,10-perylenebis-

(dicarboximide) are synthesised using the procedure described in Ref. 23, a slightly modified version of the procedure reported in Refs. 19 and 22. For the chiral sample (chiral-PDI), one starting compound is (S)-(-)-2-amino- methyl-1-ethylpyrrolidine, and for the racemic sample (racemic-PDI) 2-aminomethyl-1-ethylpyrrolidine is used (both obtained from Sigma-Aldrich). Since there are two chiral centers on each molecule, the chiral-PDI is the SS isomer and the racemic-PDI is a mixture of four isomers of equal concentration; two are chiral enantiomers (the SS and RR isomers) and two are achiral enantiomers (the SR and RS isomers). The SR and RS isomers are actually the same molecule. The structure of these isomers as HCl salts are shown in Fig. 1 and Fig. S1 of the Electronic Supplementary Information. In order to form chiral-PDI-HCl and racemic-PDI-HCl, 12 wt% mixtures of chiral- and racemic-PDI are made with stoichiometric concentrations of reagent grade hydrochloric acid in Millipore water. The total concentration of chiral- and racemic-PDI-HCl is kept at 12 wt%, but the proportions of chiral- and racemic-PDI-HCl are varied. The chiral fraction is defined as the mass of chiral-PDI-HCl divided by the sum of the masses of chiral- and racemic-PDI-HCl.

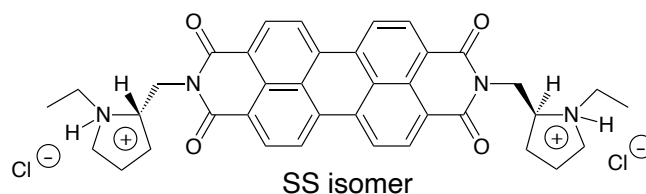


Fig. 1 SS isomer of the HCl salt of chiral-PDI. See Fig. S1 of the Electronic Supplementary Information for structures of the other isomers.

The transition temperatures of chromonic liquid crystals are very sensitive to concentration. This provides a nice check on both the purity of the synthesized products and the concentration of prepared samples. Sigma-Aldrich quotes the purity of the chiral- and racemic starting compounds as 96 and 97%, respectively. Given the synthesis procedures, the impurities in the product are likely to be these starting compounds. Both of these are soluble in methanol and ethyl acetate, and therefore are eliminated by thorough washing of the product. This is borne out by the fact that multiple syntheses of both chiral- and racemic-PDI produced samples with liquid crystal transition temperatures within 1°C of each other and consistent with the literature value.<sup>19</sup>

All mixtures were heated to between 60 and 70°C and repeatedly shaken and vortexed until all the solid dissolved. The same heating and shaking/vortexing procedure was performed for roughly a half hour before loading the mixtures into 300 μm (inside dimension) square capillaries using suction filling. Immediately after filling, the capillary was sealed with epoxy and fixed to a microscope slide. A square capillary instead of a thinner rectangular capillary was used to prevent the planar texture from forming instead of the fingerprint texture. This was most necessary for the lower chiral fraction samples. Measuring the pitch of chiral chromonic LCs using the fingerprint texture produces results consistent with other methods, e.g., the Cano wedge technique,<sup>29</sup> and is the method of choice when proper alignment at

the surfaces cannot be achieved (as is the case for chiral-PDI-HCl).

Two polarizing microscopes were utilized for the pitch measurements. For the samples with longer pitch, a Leitz Laborlux 12 Pol microscope equipped with a Zeiss AxioCam ICc 1 camera was sufficient to resolve the fingerprint texture. Images were taken using ZEN software with a 25X objective and a Instec HC5302 heating stage. For the shorter pitch samples, a Zeiss Axio Imager 2 microscope with a 50X objective, Hamamatsu ORCA-Flash4.0 V3 camera, and ZEN software were used with a Linkum LTS420 hot stage. The sample was first heated into the isotropic phase and then allowed to cool at about 5 °C/min to below room temperature. Measurements of the pitch were then performed at 5 °C intervals between 15 and 45 °C. At each temperature, several images were taken and multiple measurements of the pitch were made by using Zen software to determine the repeat distance across a straight section of the fingerprint texture (the pitch is twice the repeat distance). Only regions of the fingerprint texture that were near the capillary surface on the side of the objective and came into and out of focus as a unit were selected for measurements. The average and standard deviation of the mean for 3 - 5 locations were then calculated at each temperature. Typical images of the fingerprint texture are shown in Fig. 2.

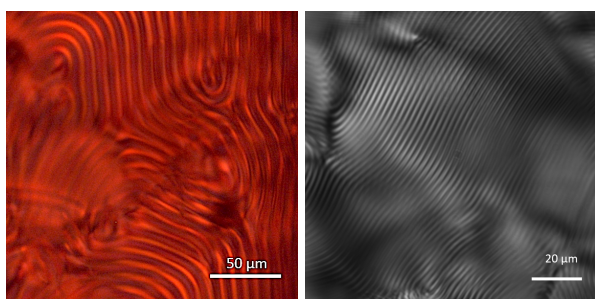


Fig. 2 Polarized optical microscopy images of the fingerprint texture using crossed polarizers. The left-hand image is for a 0.2 chiral fraction PDI-HCl sample at 45 °C using the Leitz microscope. The right-hand image is for a 0.6 chiral fraction PDI-HCl sample at 30 °C using the Zeiss microscope.

The chiral nematic to coexistence region transition temperature and the coexistence region to isotropic transition temperature were measured by heating the sample at 1 °C/min and noting the temperatures of the first appearance of the isotropic phase and the final disappearance of the chiral nematic phase.

### 3 Experimental results

Data on the inverse pitch are displayed in Fig. 3. Notice that the inverse pitch increases with chiral fraction and decreases with temperature. A linear dependence on temperature for each chiral fraction is consistent with the data if measurement uncertainties are taken into account.

As expected, the racemic sample does not show a fingerprint texture. In fact, suction filling the viscous fluid homogeneously aligns the director. As can be seen in the images of Fig. 4, there is almost no variation of the director throughout the sample, and certainly no evidence at all for a twist of any kind. Also, no optical activity was detected during a careful investigation of this 300

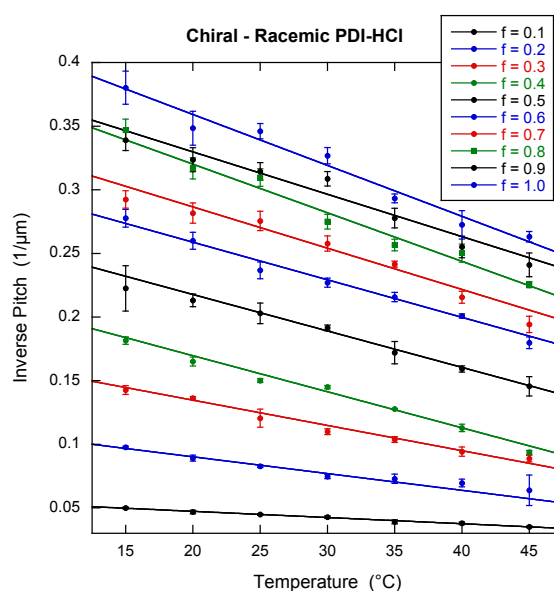


Fig. 3 Inverse pitch as a function of temperature for different chiral fractions, with the chiral fraction increasing from bottom to top. The total concentration of racemic- and chiral-PDI-HCl is 12 wt% for all chiral fractions. The lines are weighted linear least squares fits to the data.

μm thick sample. A chiral nematic with a pitch of 600 μm would fit between the sides of the capillary with the director oriented in the same direction on both surfaces. Since this is not what is observed, the pitch must be longer than that. With no evidence at all for twist, an upper limit of the pitch of the racemic sample is set at 1000 μm, yielding an inverse pitch determination of  $(0.000 \pm 0.001) \mu\text{m}^{-1}$ .

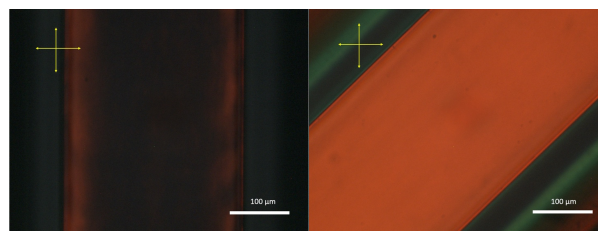


Fig. 4 Polarized optical microscopy images of the racemic sample in a 300 μm square capillary using the Leitz microscope. The left-hand image is with the capillary axis parallel to one of the crossed polarizers (shown as yellow arrows). The right-hand image is with the capillary axis at an angle of 45° to the crossed polarizers.

Additional and slightly speculative evidence that the pitch of the racemic-PDI-HCl is extremely large comes from a comparison of the isotropic droplets formed by racemic-PDI-HCl and formed by an achiral perylenetetracarboximide salt. This is discussed in the Electronic Supplemental Information.

The inverse pitch measurements as a function of chiral fraction are shown in Fig. 5 (see Fig. S3 of the Electronic Supplementary Information for an expanded view). The data at each temperature show a linear dependence with chiral fraction, although it is clear that the scatter in the data points is larger than the error estimates. This is probably due to total PDI-HCl concentrations

slightly different from 12 wt% for the different chiral fractions. The mixing process produces samples within 0.05 wt% and 0.001 of the desired total PDI-HCl concentration and chiral fraction, respectively. But even at 60 to 70°C the sample is quite viscous. Thus the process of loading and sealing the capillaries at these elevated temperatures may result in small variations in the total PDI-HCl concentration due to evaporation. Chromonic liquid crystals are very sensitive to concentration, so any small differences in concentration can explain the increased scatter of the data in Fig. 5 compared to Fig. 3.

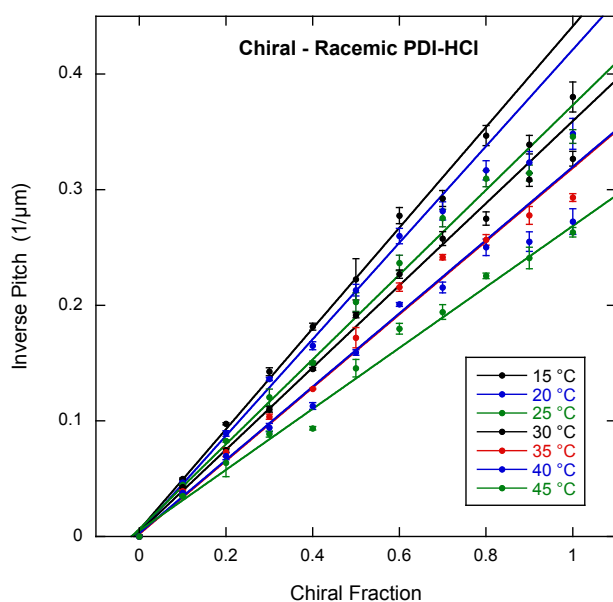


Fig. 5 Inverse pitch as a function of chiral fraction for seven different temperatures, with the temperature increasing from top to bottom (see Fig. S3 of the Electronic Supplementary Information for an expanded view of the entire plot). The total concentration of racemic- and chiral-PDI-HCl is 12 wt% for each chiral fraction. The lines are weighted linear least squares fits to the data. The slopes and intercepts of these fits are plotted in Fig. S4 of the Electronic Supplementary Information.

Measurements of the transition temperatures are shown in Fig. 6, where the error estimates indicate the typical variation observed within the same capillary. Notice that the scatter in the data is larger than the error estimates. This is strong evidence that the total PDI-HCl concentration of each prepared sample varied slightly from 12 wt% and is responsible for some of the scatter in the inverse pitch versus chiral fraction data. The transition temperature data also show a slight tendency to increase as the chiral fraction is increased, more so for the upper limit of the coexistence region than the lower limit. To our knowledge, no investigations of transition temperatures in chiral-racemic lyotropic systems are reported in the literature. In thermotropic chiral-racemic systems, transition temperatures do not depend on chiral fraction, except for the unusual case in which new liquid crystal phases occur at high chiral fraction, e.g., the blue phases.<sup>30</sup> Thus the small increase in transition temperatures in Fig. 6 is most likely due to a slight difference in the purity of the chiral- and racemic-PDI compounds used in this investigation.

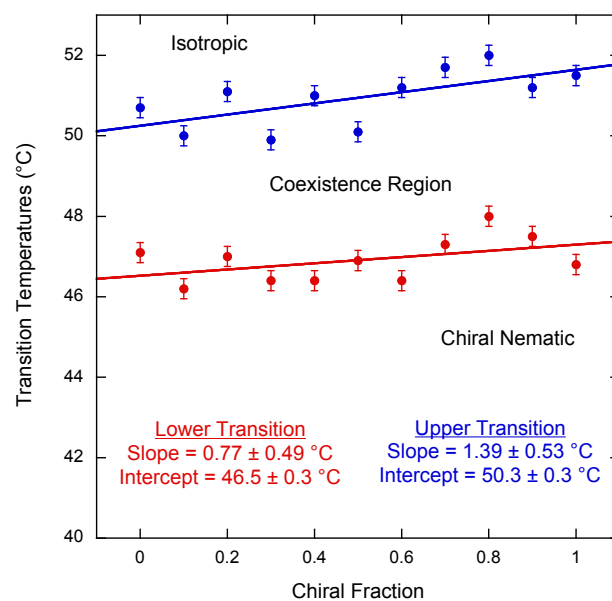


Fig. 6 Transition temperatures as a function of chiral fraction. The lines are unweighted linear least squares fit to the data with the slopes and intercepts given in the lower portion of the figure.

## 4 Discussion

The helical twisting power (HTP) is defined as

$$HTP = (1/P)/X, \quad (1)$$

where  $(1/P)$  is the inverse pitch and  $X$  is the concentration. Various units are used for  $X$ , typically mole fraction, mol%, or wt%. To make it easier to compare HTP values with other reports and to make it clear which concentration unit is being used,  $\mu\text{m}^{-1}\text{mol}\%^{-1}$  is chosen as the HTP unit. Normally HTP is calculated from the slope of the inverse pitch versus concentration data for a concentration range for which the data follow a linear relationship. Thus based on experiment, the helical twisting power of the chiral enantiomer can be derived from the slope of the data at each temperature in Fig. 5 by simply dividing the slope by  $X_{12\text{wt}\%} = 0.357 \text{ mol}\%$ , the mol% of a 12 wt% sample. As can be seen from Fig. 7, the HTP decreases with temperature between 15 and 45°C. The slope of the HTP data gives this temperature dependence, which is  $(-1.5 \pm 0.1) \times 10^{-2} (\mu\text{m}^{-1}\text{mol}\%^{-1})/^\circ\text{C}$ . Since an increase in pitch with temperature has been observed for PDI-HCl with a chiral fraction of 1,<sup>20,23</sup> a negative slope is expected. In fact, the inverse pitch of PDI-HCl with a chiral fraction of 1 decreases by around 24% over a 25°C temperature increase,<sup>23</sup> which is similar to the 38% decrease over 30°C for the helical twisting power.

Although the fits to the inverse pitch data come very close to being zero at a chiral fraction of zero, they all have a slight positive value (see Fig.S4 of the Electronic Supplementary Information). The mean of these values for all temperatures is  $0.004 \mu\text{m}^{-1}$  with a standard deviation of  $0.002 \mu\text{m}^{-1}$ . This non-zero value is most likely due to the scatter in the data due to the aforementioned slightly different total PDI-HCl concentrations of the chiral frac-

tion samples and/or the slight trend in transition temperatures as the chiral fraction is varied.

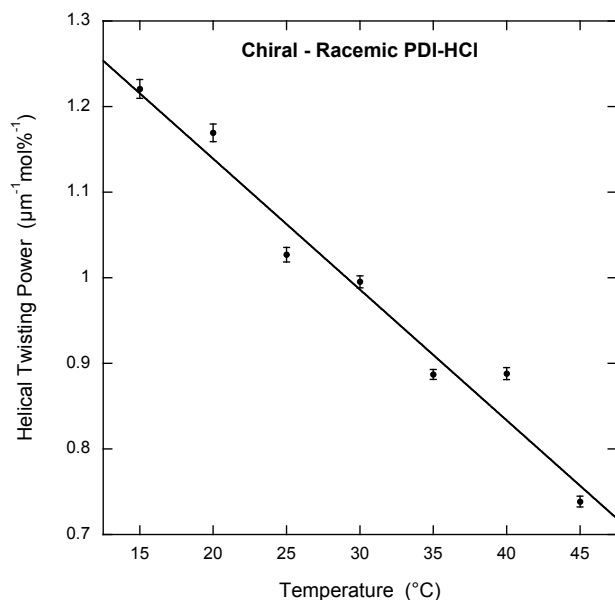


Fig. 7 Helical twisting power as a function of temperature. The data points are derived from the fits in Fig. 4 as explained in the text. The line is an unweighted linear least squares fit to the data, yielding a temperature dependence of the HTP equal to  $(-1.5 \pm 0.1) \times 10^{-2} (\mu\text{m}^{-1}\text{mol}\%^{-1})/^{\circ}\text{C}$ .

It is interesting to compare the HTP of the chiral-racemic PDI-HCl system ( $\sim 1.1 \mu\text{m}^{-1}\text{mol}\%^{-1}$  at room temperature) to other lyotropic chiral nematics. The only other studied chromonic liquid crystal composed of a chiral molecule is a chiral derivative of di-sodium cromoglycate (DSCG), for which the HTP is measured to be  $0.14 \mu\text{m}^{-1}\text{mol}\%^{-1}$  at room temperature.<sup>21</sup> The fact that the HTP values differ by almost an order of magnitude forces one to ask what is so different between the two systems. The concentration of chiral-DSCG in the experiment is 50% higher than the concentration of chiral-PDI-HCl in this experiment, so that doesn't answer the question. One interesting comparison is that the chiral-DSCG molecule has one chiral group whereas the chiral-PDI-HCl molecule has two, so perhaps that explains some of the HTP difference. But the most noteworthy difference between the two systems is the scission energy, *i.e.*, the free energy change for a molecule leaving an assembly. This parameter has not been measured for either of these chiral compounds, but it has been measured for achiral compounds with the same molecular core structure ( $\sim 7 k_B T$  for achiral DSCG and  $\sim 20 k_B T$  for an achiral perylenetetracarboximide salt, where  $k_B$  is the Boltzmann constant and  $T$  is the absolute temperature).<sup>31,32</sup> The scission energy is perhaps the most important parameter for a chromonic system undergoing quasi-isodesmic assembly and the value of  $\sim 20 k_B T$  is one of the highest measured for chromonic LCs. It directly describes the interaction strength between neighboring molecules in an assembly and indirectly determines the average assembly length and hence the nematic order parameter. With such a high scission energy, the chiral contributions to the molecular interactions in the PDI-HCl system are quite strong and therefore the

helical twisting power is very large.

There have been two studies of chiral micellar lyotropic liquid crystals, both investigating the potassium salts of acylated amino acids. The room temperature HTP is found to be between  $0.17$  and  $0.46 \mu\text{m}^{-1}\text{mol}\%^{-1}$  for three different compounds in one of these reports,<sup>13</sup> and  $0.32$  and  $0.20 \mu\text{m}^{-1}\text{mol}\%^{-1}$  for two compounds in the other report.<sup>28</sup> Clearly the HTP of the chiral-racemic PDI-HCl system is significantly greater than both of these.

The HTP of dopants added to achiral lyotropic nematics are also less than the HTP of the chiral-racemic PDI-HCl system. For the achiral chromonic liquid crystal DSCG, the largest reported room temperature HTP is for the dopant L-arginine hydrochloride at  $\sim 0.52 \mu\text{m}^{-1}\text{mol}\%^{-1}$ ,<sup>29</sup> while the HTPs for other chiral dopants are significantly less.<sup>33,34</sup> In one report on the HTP of a variety of chiral dopants in achiral micellar liquid crystals, the largest HTP is for tomatine in a cesium-perfluoro system, for which the HTP is  $0.32 \mu\text{m}^{-1}\text{mol}\%^{-1}$ .<sup>35</sup>

## 5 Conclusions

The pitch behavior of a chiral-racemic lyotropic chromonic liquid crystal system is investigated. Over a range of temperatures in the chiral nematic phase, the inverse pitch depends linearly on the chiral fraction. The helical twisting power of this system is significantly larger than for other lyotropic chiral nematic liquid crystals (both chromonic and micellar) and linearly decreases with an increase in temperature.

## Conflicts of interest

There are no conflicts to declare.

## Acknowledgements

This work was partially supported by the National Science Foundation through the University of Pennsylvania Materials Research Science and Engineering Center (MRSEC), Grant No. DMR11-20901 and DMR17-20530, including the MRSEC Optical Microscopy Experimental Central Facility. J. A. acknowledges research support from Swarthmore College. The authors thank Sophie Ettinger, Robert Paley, and Liliya Yatsunyk for their valuable assistance.

## Notes and references

- 1 L. Tortora and O. D. Lavrentovich, *Proc. Natl. Acad. Sci. U.S.A.*, 2011, **108**, 5163–5168.
- 2 J. Jeong, Z. S. Davidson, P. J. Collings, T. C. Lubensky and A. G. Yodh, *Proc. Natl. Acad. Sci. U.S.A.*, 2014, **111**, 1742–1747.
- 3 Z. S. Davidson, L. Kang, J. Jeong, T. Still, P. J. Collings, T. C. Lubensky and A. G. Yodh, *Phys. Rev. E*, 2015, **91**, 050501–1–050501–5.
- 4 K. Nayani, R. Chang, J. Fu1, P. W. Ellis, A. Fernandez-Nieves, J. O. Park and M. Srinivasarao, *Nat. Commun.*, 2015, **6**, 8067–8073.
- 5 C. F. Dietrich, P. Rudquist, K. Lorenz and F. Giesselmann, *Langmuir*, 2017, **33**, 5852–5862.
- 6 R. Chang, *PhD thesis*, Georgia Institute of Technology, 2018.

- 7 L. Lucchetti, T. P. Fraccia, G. Nava, T. Turiv, F. Ciciulla, L. Bethge, S. Klussmann, O. D. Lavrentovich and T. Bellini, *ACS Macro Lett.*, 2020, **9**, 1034–1039.
- 8 C. F. Dietrich, P. J. Collings, T. Sottmann, P. Rudquist and F. Giesselmann, *Proc. Natl. Acad. Sci. USA*, 2020, **117**, 27238–27244.
- 9 E. T. Samulski and A. V. Tobolsk, *Liquid Crystals and Ordered Fluids*, Springer, Boston, 1970, pp. 111–121.
- 10 K. Radley and A. Saupe, *Mol. Phys.*, 1978, **35**, 1405–1412.
- 11 M. Accimis and L. W. Reeve, *Can. J. Chem.*, 1980, **58**, 1533–1541.
- 12 M. R. Alcantara, M. V. M. C. de Melo, V. R. Paoli and J. A. Vanin, *Mol. Cryst. Liq. Cryst.*, 1983, **90**, 335–341.
- 13 P. S. Covello, B. J. Forrest, M. E. M. Helene, L. W. Reeves, and M. Vlst, *J. Phys. Chem.*, 1983, **87**, 176–181.
- 14 M. R. Alcantara, M. V. M. C. de Melo, V. R. Paoli and J. A. Vanin, *Mol. Cryst. Liq. Cryst.*, 1984, **107**, 303–310.
- 15 K. Radley and A. S. Tracy, *Can J. Chem.*, 1985, **63**, 95–99.
- 16 K. Radley and H. Cattey, *Mol. Cryst. Liq. Cryst.*, 1994, **250**, 167–175.
- 17 M. Boidart, A. Hochapfel and P. Peretti, *Mol. Cryst. Liq. Cryst.*, 1989, **172**, 147–150.
- 18 K. Hiltrop, *Chirality in Liquid Crystals*, Springer-Verlag, New York, 2001, ch. 14, pp. 447–480.
- 19 J. J. Naidu, Y. J. Bae, K. U. Jeong, S. H. Lee, S. Kang and M. H. Lee, *Bull. Korean Chem. Soc.*, 2009, **30**, 935–937.
- 20 L. P. Joshi, *PhD thesis*, Kent State University, 2009.
- 21 S. Yang, B. Wang, D. Cui, D. Kerwood, S. Wilkens, J. Han and Y. Y. Luk, *J. Phys. Chem. B*, 2013, **117**, 7133–7143.
- 22 R. Kularatne, H. Kim, M. Ammanamanchi, H. N. Hayenga and T. H. Ware, *Chem. Mater.*, 2016, **28**, 8489–8492.
- 23 T. Ogolla, R. S. Paley and P. J. Collings, *Soft Matter*, 2019, **15**, 109–115.
- 24 E. Akpınar, G. Topcu, D. Reis and A. M. F. Neto, *J. Mol. Liq.*, 2020, **318**, 114010–1–114010–9.
- 25 G. Zanchetta, F. Giavazzia, M. Nakata, M. Buscaglia, R. Cerbino, N. A. Clark and T. Bellini, *Proc. Natl. Acad. Sci. U.S.A.*, 2010, **107**, 17497–17502.
- 26 J. P. F. Lagerwall, C. Schütz, M. Salajkova, J. H. Noh, J. H. Park, G. Scalia and L. Bergström, *NPG Asia Mater.*, 2014, **6**, e80.
- 27 J. Lydon, *Handbook of Liquid Crystals*, Wiley-VCH, Weinheim, 2014, vol. 6, ch. 14, pp. 439–483.
- 28 E. Akpınar, F. Giesselmann and M. Acimis, *Liq. Cryst.*, 2013, **40**, 1183–1194.
- 29 T. Ogolla, S. B. Nashed and P. J. Collings, *Liq. Cryst.*, 2017, **44**, 1968–19784.
- 30 D. K. Yang and P. P. Crooker, *Phys. Rev. A*, 1987, **35**, 4419–4423.
- 31 A. J. Dickinson, N. D. LaRacuenta, C. B. McKitterick and P. J. Collings, *Mol. Cryst. Liq. Cryst.*, 2009, **509**, 9–20.
- 32 T. Ogolla and P. J. Collings, *Liq. Cryst.*, 2019, **46**, 1551–1557.
- 33 H. Lee and M. M. Labes, *Mol. Cryst. Liq. Cryst.*, 1982, **84**, 137–157.
- 34 H. Lee and M. M. Labes, *Mol. Cryst. Liq. Cryst.*, 1984, **108**, 125–132.
- 35 M. Pape and K. Hiltrop, *Mol. Cryst. Liq. Cryst.*, 1997, **307**, 1155–173.